

# Number of Multipath Clusters in Indoor MIMO Propagation Environments

Nicolai Czink, Markus Herdin, Hüseyin Özcelik, Ernst Bonek

*Abstract:* An essential parameter of physical, propagation based MIMO channel models is the number of multipath clusters. In this paper we determine the *total* number of clusters and the number of *dominant* clusters in the angle-of-arrival/angle-of-departure domain based on comprehensive indoor MIMO measurements at 5.2 GHz in a cluttered office environment. For the *dominant* multipath clusters we find a mean number of 7.6 with a standard deviation of 2.4, whereas the *total* number of clusters varies strongly even within a single room of the environment.

*Introduction:* The use of multiple antennas at both link ends (MIMO) in wireless communications promises high spectral efficiency and reliability. Accurate channel models are required for proper design of signal processing algorithms. One important parameter is the number of (dominant) multipath clusters. There are various definitions of “clusters” (e.g. [1]). The most accurate definition would be a group of multi-path components with similar angle-of-arrival (AoA), angle-of-departure (AoD), and delay. As

we are concentrating only on the AoA/AoD-plane, we disregard the delay in this paper. Previous results on the number of multipath clusters were obtained only for single-input multiple-output (SIMO) channels in the AoA/delay-domain, except for [2]. Using SAGE estimates to identify the number of clusters, the authors of [1] are showing an average number of 7 clusters. Other than the mean, there is no statistical information provided. Using a spatial filter on SAGE estimates, Kai Yu et al. [3] obtained 4 to 5 clusters on average. In [4] an average number of 3 to 4 clusters was observed with limited angular resolution. Haneda et al. [2] consider only two environments, but map the clusters to physical scatterers.

Based on a comprehensive indoor MIMO measurement campaign we investigate the number of multipath clusters in the joint AoA/AoD-domain.

*Measurement set-up and scenario:* MIMO channel matrices were measured at the Institut für Nachrichtentechnik und Hochfrequenztechnik, Technische Universität Wien, at 5.2 GHz. At transmit side (Tx), we used a single positionable sleeve antenna to form a  $20 \times 10$  virtual rectangular array with an inter-element spacing of  $\lambda/2$ . At the receiver (Rx), a directional linear array of printed dipoles with 8 elements, spaced  $0.4\lambda$  and with a  $120^\circ$  3dB field-of-view each, was used. The channel was probed at 193 equi-spaced frequency bins over 120 MHz of bandwidth. The virtual transmit array was positioned in a hallway. The receiver was deployed at 24 different positions (“scenarios”) in several offices connected to this hallway. On each position, the receiver was looking in 3 different directions (rotated by  $120^\circ$ ), which were combined afterwards for our investigations to gain a field-of-view of  $360^\circ$ . Except one position/direction we measured only NLOS

scenarios. A more detailed measurement description can be found in [5].

*Evaluation:* For each Rx position and direction, we created different spatial realisations of the  $8 \times 8$  MIMO channel matrix  $\mathbf{H}_i$ , where  $i$  denotes the  $i$ th spatial realisation. This was done by moving a virtual 8-element uniform linear array (ULA) over the  $20 \times 10$  Tx grid and resulted in  $N = 130$  spatial realisations. To save computation time, only one frequency bin was used for measurement evaluation. Comparative evaluations have shown that the number of multipath clusters did not change when using more frequency bins, as there are enough spatial realisations to mitigate frequency selective fading.

For each position and direction, the double-directional angular power spectrum (APS) [6] was calculated using the Bartlett beamformer [7] by<sup>1</sup>

$$P(\varphi_{\text{Rx}}, \varphi_{\text{Tx}}) = (\mathbf{a}_{\text{Tx}}(\varphi_{\text{Tx}}) \otimes \mathbf{a}_{\text{Rx}}(\varphi_{\text{Rx}}))^H \mathbf{R}_{\mathbf{H}} ((\mathbf{a}_{\text{Tx}}(\varphi_{\text{Tx}}) \otimes \mathbf{a}_{\text{Rx}}(\varphi_{\text{Rx}})), \quad (1)$$

where  $\mathbf{a}_{\text{Rx}}(\varphi_{\text{Rx}})$  denotes the normalised response vector from AoA,  $\varphi_{\text{Rx}}$ , relative to the array broadside, and  $\mathbf{a}_{\text{Tx}}(\varphi_{\text{Tx}})$  the normalised steering vector for AoD,  $\varphi_{\text{Tx}}$ .

The full spatial correlation matrix,  $\mathbf{R}_{\mathbf{H}}$ , was estimated by<sup>1</sup>

$$\mathbf{R}_{\mathbf{H}} = \frac{1}{N} \sum_{i=1}^N \text{vec}(\mathbf{H}_i) \text{vec}(\mathbf{H}_i)^H. \quad (2)$$

The APS for the three different receive array directions were combined to a full  $360^\circ$  power spectrum and normalised afterwards, such that the strongest peak of the combined APS had 0dB.

---

<sup>1</sup> $(\cdot)^H$  denotes hermitian transpose,  $\otimes$  denotes the Kronecker product, the  $\text{vec}(\cdot)$  operator stacks a matrix into a vector columnwise

The main drawback of the Bartlett APS is its high side-lobes. Hence, we used the SAGE super-resolution algorithm [8] (implementation from [9]) to estimate the set of complex amplitude, AoA, and AoD, from each realisation  $\mathbf{H}_i$ . A model order of 10 (which corresponds to the 10 strongest paths of each channel realisation) was chosen because the visualization produced best results, using the algorithm we will describe presently. This leads to a total number of  $10 \times 130 = 1300$  estimates per position and direction.

The resolvable dynamic range per position and direction was 30 dB. As powers in different directions can vary, only such components with powers not more than 30 dB below the strongest peak in the combined APS were regarded in the identification of clusters. A cluster was defined to be “*dominant*” if its power was not more than 10 dB below the power of the strongest cluster, so there is at least one dominant cluster in a scenario.

To identify the multipath clusters per scenario visually, we plotted the Bartlett and SAGE estimates overlaid. In some cases it turned out that clusters were well separated in the Bartlett APS. There, the APS was sufficient to identify the number of clusters, SAGE estimates were only used for verification. In scenarios where clusters were very close to each other, it was not possible to separate them by the Bartlett APS. There, cluster separation was solely based on SAGE estimates. In that case, clusters were identified by dense SAGE estimation points in the AoA/AoD-plane. Isolated estimates were disregarded to avoid errors at the lower limit of the dynamic range. In some scenarios, the SAGE estimates were spread widely and could not be used for verification or identification, in this case, only the Bartlett APS was used.

*Results:* Figure 1 shows the APS of an exemplary rich scattering scenario (light colours indicate strong powers), overlaid with SAGE estimates (white dots). The visually identified multipath clusters are marked by black circles. Here, the Bartlett beamformer provides sufficient information about the number of clusters in principle, but it tends to overestimate this number because of side-lobe effects (e.g. AoA/AoD:  $130^\circ/18^\circ$ ). Therefore, SAGE estimates are used for verification of the results. This scenario exhibits 24 multipath clusters with 2 dominant clusters.

The normalised histogram (hist) of the number of *dominant* multipath clusters ( $N_{C,\text{dom}}$ ) and the *total* number of multipath clusters ( $N_{C,\text{tot}}$ ) for all 24 considered scenarios are shown in Figures 2 and 3, respectively.

Figure 2 shows that  $N_{C,\text{dom}} = 7$  *dominant* clusters are most probable, with a mean value of 7.6 and an empirical standard deviation of 2.4. Figure 3 shows the normalised hist of the *total* number of clusters. The total number of clusters varies very strongly (between 6 and 31 in our environment), even for scenarios which were gathered in the same room. A total number of 24 or 25 clusters were most probable, with a mean value of 21.3 and an empirical standard deviation of 6.1. However, in scenarios with a large number of multipath clusters, most of those clusters had very low power.

*Conclusions:* Based on a comprehensive indoor MIMO measurement campaign we investigated the number of multipath clusters in a cluttered office environment. We applied a new method based on the Bartlett and SAGE estimates of the APS for identifying clusters in the AoA/AoD-domain. We found a number of 7 *dominant* clusters to be most likely with a mean value of 7.6 in the measured office environment. For a dynamic

range of 30 dB, the *total* number of clusters varies strongly.

*Acknowledgements:* We thank Helmut Hofstetter (ftw.) for help with the measurements, T-Systems Nova GmbH for providing the receive antenna array, and Sven Semmelrodt of University of Kassel for providing the SAGE implementation.

## References

- [1] C.-C. Chong, C.-M. Tan, D. Laurenson, S. McLaughlin, M. Beach, and A. Nix, “A new statistical wideband spatio-temporal channel model for 5-GHz band WLAN systems,” *IEEE Journal on Selected Areas in Communications*, vol. 21, no. 2, pp. 139 – 150, Feb. 2003.
- [2] K. Haneda, J. Takada, and T. Kobayashi, “Clusterization analysis of spatio-temporal UWB radio channel for line-of-sight and non-line-of-sight indoor home environments,” Joint COST 273/284 Workshop on Antennas and Related System Aspects in Wireless Communications, June 2004, Gothenburg, Sweden.
- [3] K. Yu, Q. Li, D. Cheung, and C. Prettie, “On the tap and cluster angular spreads of indoor wlan channels,” in *Proceedings of IEEE Vehicular Technology Conference Spring 2004*, Milano, Italy, May 17–19, 2004.
- [4] Q. H. Spencer, B. D. Jeffs, M. A. Jensen, and A. L. Swindlehurst, “Modeling the statistical time and angle of arrival characteristics of an indoor multipath channel,” *IEEE Journal on Selected Areas in Communications*, vol. 18, pp. 347 – 359, March 2000.

- [5] H. Özcelik, M. Herdin, R. Prestros, and E. Bonek, “How MIMO capacity is linked with single element fading statistics,” in *Proc. International Conference on Electromagnetics in Advanced Applications*, Torino, Italy, September 2003, pp. 775–778.
- [6] M. Steinbauer, A. Molisch, and E. Bonek, “The double-directional radio channel,” *IEEE Antennas and Propagation Magazine*, vol. 43, no. 4, pp. 51 – 63, Aug. 2001.
- [7] M. Bartlett, “Smoothing periodograms from time series with continuous spectra,” *Nature*, vol. No. 161, 1948.
- [8] B. H. Fleury, M. Tschuddin, R. Heddergott, D. Dahlhaus, and K. I. Pedersen, “Channel parameter estimation in mobile radio environments using the SAGE algorithm,” *IEEE J. Sel. Areas Comm.*, vol. 18, no. 3, pp. 434–450, March 1999.
- [9] S. Semmelrodt, R. Kattenbach, and H. Früchting, “Toolbox for spectral analysis and linear prediction of stationary and non-stationary signals,” COST 273 TD(04)019, Athens, Greece, January 26-28, 2004.

**Authors’ affiliations:**

N. Czink, M. Herdin, H. Özcelik, and E. Bonek (Institut für Nachrichtentechnik und Hochfrequenztechnik, TU-Wien Gusshausstrasse 25/389, A-1040 Wien, Austria)

{nicolai.czink,markus.herdin,hueseyin.oezcelik,ernst.bonek}@tuwien.ac.at

**Figure Captions:**

Figure 1: Exemplary double-directional angular power spectrum in a cluttered office room. SAGE estimates: white dots; identified clusters: black circles.

Figure 2: Normalised histogram of the number of *dominant* multipath clusters

Figure 3: Normalised histogram of the *total* number of multipath clusters

Figure 1:

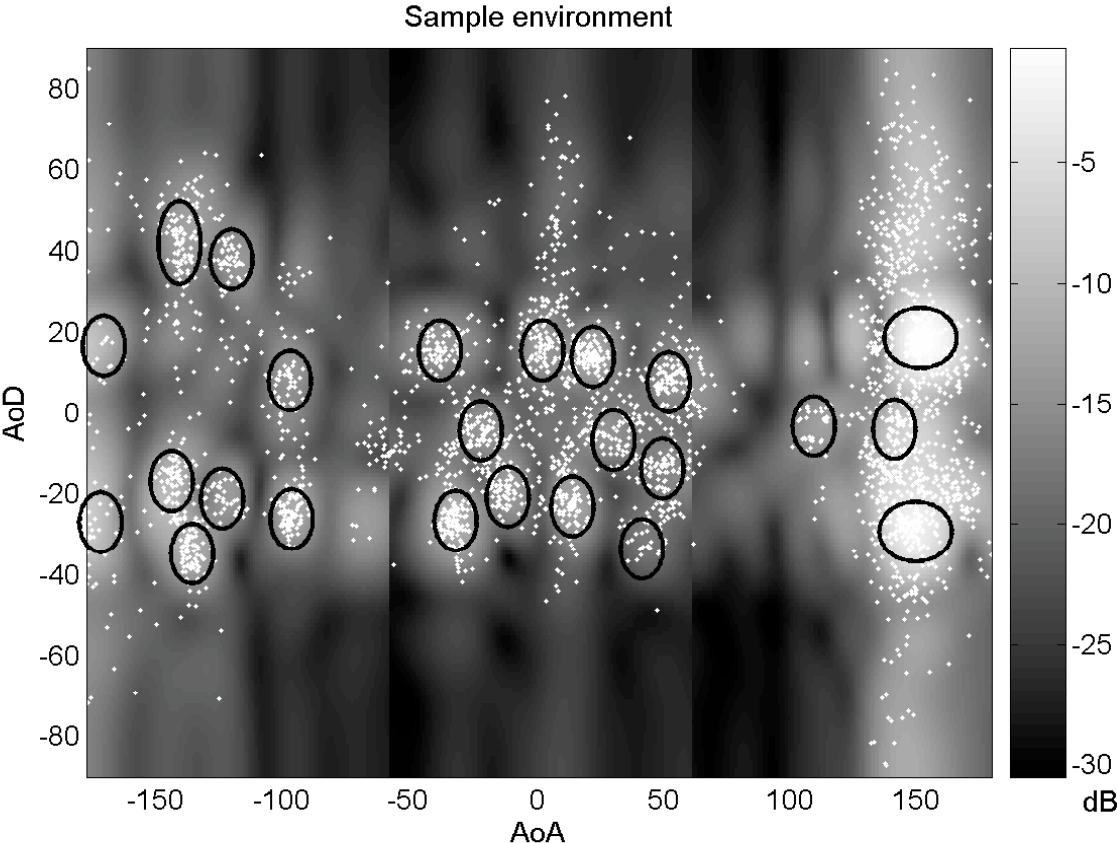


Figure 2:

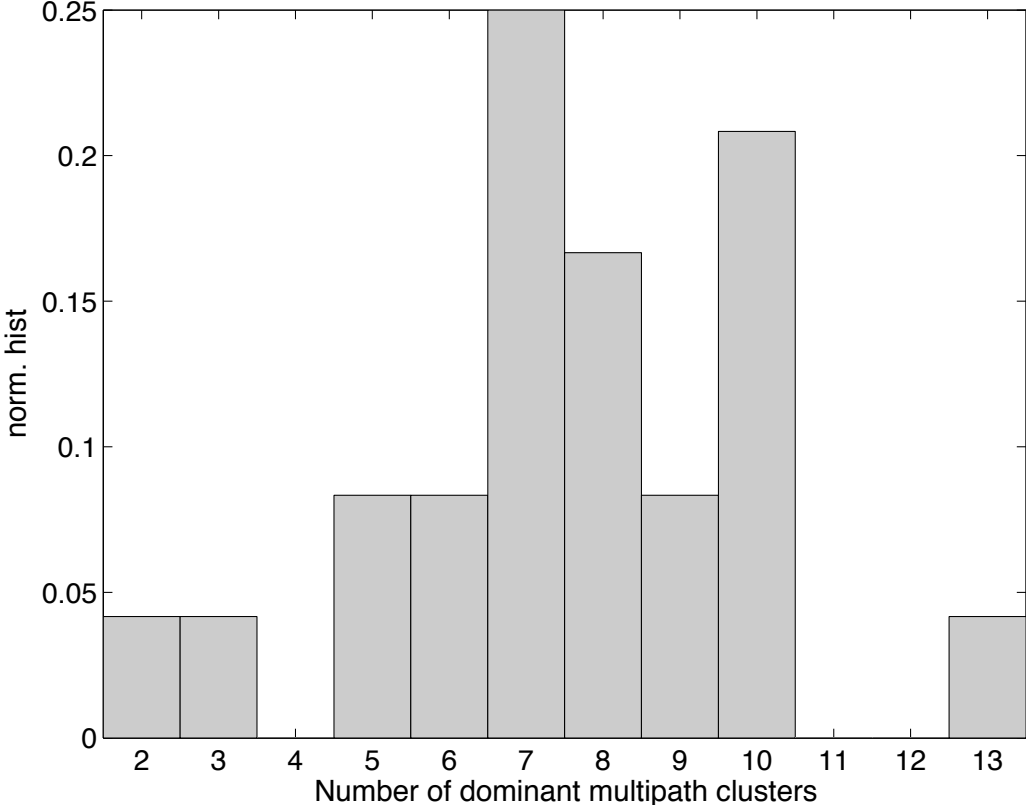


Figure 3:

